Babol University Of Medical Sciences

IJMCM, Autumn 2025, VOL 14, NO 4

International Journal of Molecular and Cellular Medicine

Journal homepage: www.ijmcmed.org

ORIGINAL ARTICLE

Synergistic Efficacy of Dual-Target HSA-Based Delivery for HER and VEGFR Co-Blockade in Triple-Negative Breast Cancer

Sadegh Rostaminasab[1], Sahar Memarkashani[1], Tahereh Rahdari[2], S. Mohsen Asghari[*2]

1. Department of Biology, Faculty of Sciences, University of Guilan, Rasht, Iran.
2. Institute of Biochemistry and Biophysics, University of Tehran, Tehran, Iran.

ARTICLE INFO

Received: 2025/09/1
Revised: 2025/11/18
Accepted: 2025/12/7

[*]**Corresponding**:
S. Mohsen Asghari
Address:
Institute of Biochemistry and Biophysics, University of Tehran, Tehran, Iran.
E-mail:
sm.asghari@ut.ac.ir

ABSTRACT

Resistance to monotherapies targeting receptor tyrosine kinases remains a major challenge in triple-negative breast cancer (TNBC). Here, we developed a dual-target HSA-based nanobioconjugate combining human serum albumin (HSA)-encapsulated lapatinib, an EGFR1/2 inhibitor**,** with the VEGFR1/2-blocking peptide VGB3 to achieve coordinated HER and VEGFR inhibition. Molecular docking predicted stable hydrogen-bonding and hydrophobic interactions between Lapatinib (free and HSA-bound) and EGFR1/2, and between VGB3 and VEGFR1/2. HSA encapsulation enabled pH-responsive, sustained drug release with faster kinetics under mildly acidic tumor conditions. Thermal denaturation assays confirmed an increase in the conformational stability of HSA after binding, indicating structural integrity and biocompatibility. In vitro studies revealed that HSA-Lapatinib exhibited a ~55 % reduction in IC_{50} (from ≈ 71 µM to ≈ 32 µM) compared with free Lapatinib. The combination of 17 µM HSA-Lapatinib and 0.18 µM VGB3 reduced cell viability to 25 % (CI = 0.29), confirming a strong synergistic effect. Flow cytometric analysis demonstrated a significant increase in apoptosis—from 40.8 % (HSA–Lapatinib) to 46.8 % (combination) ($P < 0.05$). RT-PCR further showed a fourfold upregulation of *VEGFR2* ($P < 0.0001$), supporting that HSA-Lapatinib triggers compensatory *VEGFR2* activation which is neutralized by VGB3. Collectively, these findings substantiate a mechanistic and quantitative synergy between HSA-mediated HER inhibition and VGB3-based VEGFR blockade. This dual-target HSA-Lapatinib/VGB3 system offers enhanced potency, reduced resistance, and a promising platform for precision-guided TNBC therapy.

Keywords: Triple-negative breast cancer, Human serum albumin, Lapatinib, VEGFR2 upregulation, VGB3 peptide, Dual-target therapy.

Cite this article: Rostaminasab S, et al. Synergistic Efficacy of Dual-Target HSA-Based Delivery for HER and VEGFR Co-Blockade in Triple-Negative Breast Cancer. International Journal of Molecular and Cellular Medicine. 2025; 14 (4):1031-1344. DOI: 10.22088/IJMCM.BUMS.14.4.1031

[Downloaded from ijmcmed.org on 2026-11-07]

[DOI: 10.22088/IJMCM.BUMS.14.4.1031]

© The Author(s).
Publisher: Babol University of Medical Sciences
This work is published as an open access article distributed under the terms of the Creative Commons Attribution 4.0 License (http://creativecommons.org/licenses/by-nc/4). Non-commercial uses of the work are permitted, provided the original work is properly cited.

Introduction

Triple-negative breast cancer (TNBC) is one of the most lethal subtypes of breast cancer (1), characterized by the absence of estrogen receptor (ER), progesterone receptor (PR), and HER2 expression. This aggressive phenotype is associated with rapid tumor progression and high mortality rates among women worldwide. In 2020, TNBC ranked among the leading causes of breast cancer–related deaths globally.

Over the past decades, targeted therapies have emerged as a promising approach for TNBC, using agents that selectively bind to tumor-specific proteins or receptors to limit off-target toxicity (2). Among hydrophobic chemotherapeutic agents, doxorubicin and lapatinib have shown clinical efficacy but cause serious adverse effects, including cardiotoxicity, hepatic injury, and gastrointestinal complications (3, 4). To address these issues, advanced drug-delivery platforms have been developed, with albumin-based nanocarriers representing a particularly attractive option (5-9). Human serum albumin (HSA) offers multiple advantages as a carrier: exceptional biocompatibility, high loading capacity for hydrophobic drugs, and intrinsic solubility enhancement (10). Therapeutic delivery is strengthened by albumin's dual-targeting capabilities: passive tumor accumulation via the enhanced permeability and retention (EPR) effect, and active uptake through SPARC and GP60 receptor pathways (11-13). SPARC, overexpressed in many malignancies including TNBC, binds albumin with high affinity to promote tumor-selective deposition. GP60 (albondin) facilitates transendothelial transport of albumin into tumor tissue. Acting together, SPARC functions as a tumor "homing beacon," while GP60 serves as a "molecular gateway," enabling efficient drug accumulation at the tumor site.

Combination therapy is another strategy to reduce toxicity and improve efficacy. In TNBC, co-administration of anti-angiogenic agents with targeted therapeutics has shown superior pharmacological outcomes and mitigation of drug-resistance mechanisms (14-19). Bevacizumab, a VEGF-blocking antibody, and sorafenib, a multi-target kinase inhibitor, are widely used anti-angiogenic drugs but are linked with significant side effects, such as hypertension and organ toxicity (20, 21). The VGB3 peptide is a promising anti-angiogenic agent that specifically inhibits VEGFR1 and VEGFR2, preventing tumor neovascularization (22-26). By cutting off the tumor's blood supply, VGB3 can complement existing drugs, potentially matching or exceeding the efficacy of bevacizumab or sorafenib while avoiding severe toxicity (25, 27-29). Unlike previously reported albumin-bound systems (e.g., Abraxane or HSA–Doxorubicin) that rely solely on passive accumulation, the present construct employs a dual-target strategy, in which HSA functions both as a solubilizing carrier for Lapatinib and as a targeting scaffold for co-presentation of the anti-angiogenic peptide VGB3. This design enables simultaneous HER and VEGFR blockade within a single nanobioconjugate, providing synergistic pathway inhibition rather than simple co-administration of separate agents. To our knowledge, this is the first HSA-based conjugate combining Lapatinib with a peptide VEGFR inhibitor, effectively linking improved drug delivery with suppression of compensatory signaling.

Here, we investigate this dual-target HSA–Lapatinib/VGB3 system as a means to enhance efficacy and reduce toxicity in TNBC. The approach is intended to overcome a key resistance mechanism—Lapatinib-induced VEGFR2 upregulation—through concurrent inhibition of this escape pathway. We hypothesize that such coordinated co-blockade will potentiate Lapatinib's antitumor effect and establish a rational framework for integrated drug-delivery and resistance-modulation strategies in TNBC.

Methods

Material

TheMDA-MB-231 cell line was purchased from Iran Pasteur Institute. . The procurement of the AnnexinV/PI apoptosis detection kit was purchased from BD Biosciences. The HSA (recombinant) was purchased from Sigma-Aldrich. Lapatinib ditosylate monohydrate was obtained from Sigma-Aldrich. The culture media and penicillin-streptomycin were purchased from Gibco Life Technologies. This study was approved by the ethics committee with the code IR.TUMS.TIPS.1399.104.

Peptide Synthesis

The VGB3 peptide (sequence: ECRPPDDGLC) was synthesized using the standard Fmoc solid-phase method. Purity was confirmed by high-performance

[Downloaded from ijmcmed.org on 2026-11-07]

[DOI: 10.22088/IJMCM.BUMS.14.4.1031]

liquid chromatography (HPLC), and molecular weight was verified by electrospray ionization mass spectrometry (ESI-MS).

Molecular Interaction Studies

Crystal structures of target receptors were retrieved from the RCSB PDB database: VEGFR1 (2XAC, 2.71 Å), VEGFR2 (3V2A, 3.20 Å), HER1 (1M17, 2.60 Å), HER2 (3PP0, 2.25 Å), and HSA (1E7G, 2.50 Å). Before docking, non-essential components (e.g., water molecules) were removed using Discovery Studio 2016. The VGB3 structure was modeled in Modeller 9.15.

Docking simulations for free and HSA-bound Lapatinib with HER1/HER2, and VGB3 with VEGFR1/VEGFR2, were performed. Binding energies and interaction types (hydrogen bonds, hydrophobic contacts) were analyzed using Discovery Studio and LigPlot+.

Preparation of HSA-Lapatinib Complex

Lapatinib was dissolved in dimethyl sulfoxide (DMSO) and gently mixed with HSA at a 1:1 molar ratio, stirring for 2 h at 4 °C. The DMSO content in all solutions was maintained below 1% (v/v). The mixture was dialyzed (12 kDa cut-off) against PBS (pH 7.4) to remove unbound drug and residual solvent.

Drug Loading Assessment

UV-Vis spectroscopy at 368 nm was used to determine Lapatinib concentration before and after dialysis. A calibration curve was applied to calculate loading efficiency.

PH-dependent Drug Release

Fluorescence spectroscopy (λ_em = 428 nm) monitored Lapatinib release from the HSA complex at tumor-relevant pH values (5.8, 6.3, 6.8, 7.4) over 0–72 h. A fixed concentration of 28 μM was used, ensuring no fluorescence quenching below this level.

Thermal Stability Analysis

Thermal unfolding of HSA and HSA-Lapatinib (0.003 mM) was monitored by fluorescence. Unfolding temperature (T_u), denaturation temperature (T_d), and melting temperature (T_m) were recorded to compare thermal stability.

Size Distribution and Zeta potential

The hydrodynamic size distribution and zeta potential of HSA–Lapatinib nanoparticles were measured using a Dynamic Light Scattering (DLS) analysis. Samples were diluted in deionized water before measurement to minimize multiple scattering effects. Each measurement was performed at 25 °C and repeated three times.

In Vitro Cytotoxicity (MTT Assay)

MDA-MB-231 cells (10^4 /well) were seeded in 96-well plates for 48 h, then treated for 48 h with free lapatinib, VGB3 peptide, HSA-lapatinib, or HSA-Lapatinib + VGB3 at varying concentrations. Untreated and vehicle (DMSO) groups served as controls. MTT reagent (20 μL, 5 mg/mL) was added for 4 h before solubilizing formazan with DMSO. Absorbance was read at 570 nm.

Quantitative Assessment of Drug Synergy (Chou–Talalay Model)

The interaction between HSA–Lapatinib and VGB3 peptide was quantitatively assessed using the median-effect principle established by Chou and Talalay. Briefly, MDA-MB-231 breast cancer cells were treated with increasing concentrations of free Lapatinib, HSA–Lapatinib, and VGB3, either individually or in combination, followed by 48 h incubation and viability measurement using the MTT assay. The half-maximal inhibitory concentrations (IC_{50}) were determined from nonlinear regression of dose–response curves fitted to a sigmoidal (four-parameter logistic) model. The IC_{50} values obtained were 43.76 μM for free Lapatinib, 19.52 μM for the HSA–Lapatinib complex, and 32 μM for the VGB3 peptide. For the combination study, sub-IC_{50} concentrations of HSA–Lapatinib (17 μM) and VGB3 (0.18 μM) were co-administered to the cells, resulting in 25 % viability (75 % inhibition). The Combination Index (CI) was then calculated following the Chou–Talalay equation:

$$CI_x = \frac{(D)_A}{(D_X)_A} + \frac{(D)_B}{(D_X)_B}$$

Where D_A and D_B are the doses of HSA–Lapatinib and VGB_3 in combination producing the given effect, and D_xA and D_xB are the corresponding doses of each agent alone achieving the same inhibition level. Doses D_xA and D_xB were extrapolated from the individual

[Downloaded from ijmcmed.org on 2026-11-07]

[DOI: 10.22088/IJMCM.BUMS.14.4.1031]

dose–response equations. A CI < 1 indicates synergy, CI = 1 additive effect, and CI > 1 antagonism. Under the present conditions, the calculated CI = 0.29, confirming a strong synergistic interaction between HSA–Lapatinib and VGB3. All synergy calculations were performed according to the median-effect analysis implemented in CompuSyn (ComboSyn Inc, USA).

Apoptosis Assay (Annexin V/PI)

Cells were seeded in 6-well plates, treated as above, harvested, and stained with Annexin V-FITC and propidium iodide in the dark (15 min). Flow cytometry (BD FACSCalibur™) and FlowJo v10.8.1 quantified apoptotic cells.

RNA Extraction and cDNA Synthesis

RNA was extracted using TRIzol or the RNeasy Mini Kit per the manufacturer's protocol. RNA quality was checked by NanoDrop. cDNA synthesis was performed with 1 µg RNA using the High-Capacity cDNA Reverse Transcription Kit under the following cycle: 25 °C (10 min), 37 °C (120 min), 85 °C (5 min). cDNA was stored at −20 °C.

Primer Design and qPCR

Primers for VEGFA and VEGFR2 were designed in Primer3 and validated by NCBI Primer-BLAST. All were synthesized by Macrogen (South Korea) with the following sequences:

VEGFA:
Forward:5'-TTGCCTTGCTGCTCTACCTCCA-3'
Reverse: 5'-GATGGCAGTAGCTGCGCTGATA-3'

VEGFR2:
Forward:5'-CGGACAGTGGTATGGTTCTTGC-3'
Reverse: 5'-GTGGTGTCTGTGTCATCGGAGTG-3'

qPCR was run with SYBR Green master mix on a QuantStudio system, using β2-microglobulin as the reference gene. Reactions were performed in triplicate, and relative expression was calculated using the 2^{-} ΔΔCt method.

Statistical Analysis

Data are expressed as mean ± SD from three independent replicates. One-way ANOVA with Tukey's post-hoc test was used in GraphPad Prism 9. Significance levels: *P < 0.05, **P < 0.01, ***P < 0.001, ****P < 0.0001; ns = non-significant.

Results

Molecular Interaction Studies

Albumin is a globular transport protein with three main domains (I, II, III), each containing two subdomains (A and B). The IIA and IIIA domains contain Sudlow sites 1 and 2, respectively, which are known drug-binding pockets (30, 31). Lapatinib has three reported binding sites on albumin (9), but strong interactions predominantly occur at the IB site. Docking simulations showed Lapatinib binding to the hydrophobic pocket of HSA in domain IB, forming hydrogen bonds with Arg117 and hydrophobic contacts with Met123, Tyr161, Tyr138, Phe165, Ala158, and Leu139. The binding free energy at this site was −9.3 kcal/mol (Figure 1).

Docking also revealed that Lapatinib interacts with HER1 via hydrogen bonds with Cys721 and Cys773, and with HER2 via Met801, with binding energies of −9 kcal/mol and −10 kcal/mol, respectively (Figure 2). The VGB3 peptide bound VEGFR1 through hydrogen bonds with Lys200, His223, and Lys171, and VEGFR2 through interactions with Asn274, Lys183, Ile256, Asn141, Ser311, Asp257, Lys144, and Thr139 (Figure 3). In our previous study, fluorescence quenching analysis using the Stern–Volmer equation demonstrated a static quenching mechanism between HSA and Lapatinib, with a binding constant (K_b) of 1.7×10^5 M^{-1} and a single binding site (9). Drug loading. UV-Vis absorbance at 368 nm confirmed lapatinib loading onto HSA. Before dialysis, the HSA-Lapatinib complex had an absorbance of 1.2; after dialysis, the value decreased to 0.8, corresponding to a 65% loading efficiency (Table 1).

PH-Dependent Drug Release

Fluorescence spectroscopy (428 nm emission) demonstrated negligible signal from free Lapatinib, confirming that fluorescence originated from HSA-bound drug. At pH 5.8, 6.3, and 6.8, lapatinib release was higher than at physiological pH 7.4. Release was monitored over 0–72 h, showing that acidic conditions favored drug dissociation from HSA, consistent with tumor microenvironment acidity (Figure 4).

Thermal Stability of HSA and HSA-Lapatinib

Fluorescence-based thermal denaturation analysis showed the HSA-Lapatinib complex had a melting temperature (T_m) 5.5 °C higher than free HSA. This

[Downloaded from ijmcmed.org on 2026-11-07]

[DOI: 10.22088/IJMCM.BUMS.14.4.1031]

indicates that drug binding increased structural stability and induced conformational changes in the tryptophan microenvironment (Figure 5).

Mean Size, Zeta Potential, and Polydispersity index (PDI)

According to the DLS, the mean hydrodynamic diameter of the HSA–Lapatinib complex was approximately 57 nm, with a zeta potential of -12 mV and PDI of 0.3. These values indicate a moderately stable colloidal system with uniform size distribution suitable for biological applications (Figure 6). In our previous study, TEM and AFM analyses confirmed the successful formation of HSA–Lapatinib complexes. TEM images showed an increase in particle size from 9–10 nm for free HSA to approximately 13 nm for HSA–Lapatinib, while AFM measurements revealed diameters of 8–9.5 nm and 10–11 nm for HSA and HSA–Lapatinib, respectively (9). These results verified that Lapatinib was effectively incorporated into the HSA structure without inducing aggregation or structural deformation. The size difference between DLS and microscopic (TEM/AFM) measurements is natural, as DLS reflects the hydrodynamic diameter in solution including the hydration shell and surface-bound molecules, while microscopy shows the dry core size; nevertheless, both results are consistent and mutually confirm the successful formation and stability of HSA–Lapatinib nanoparticles.

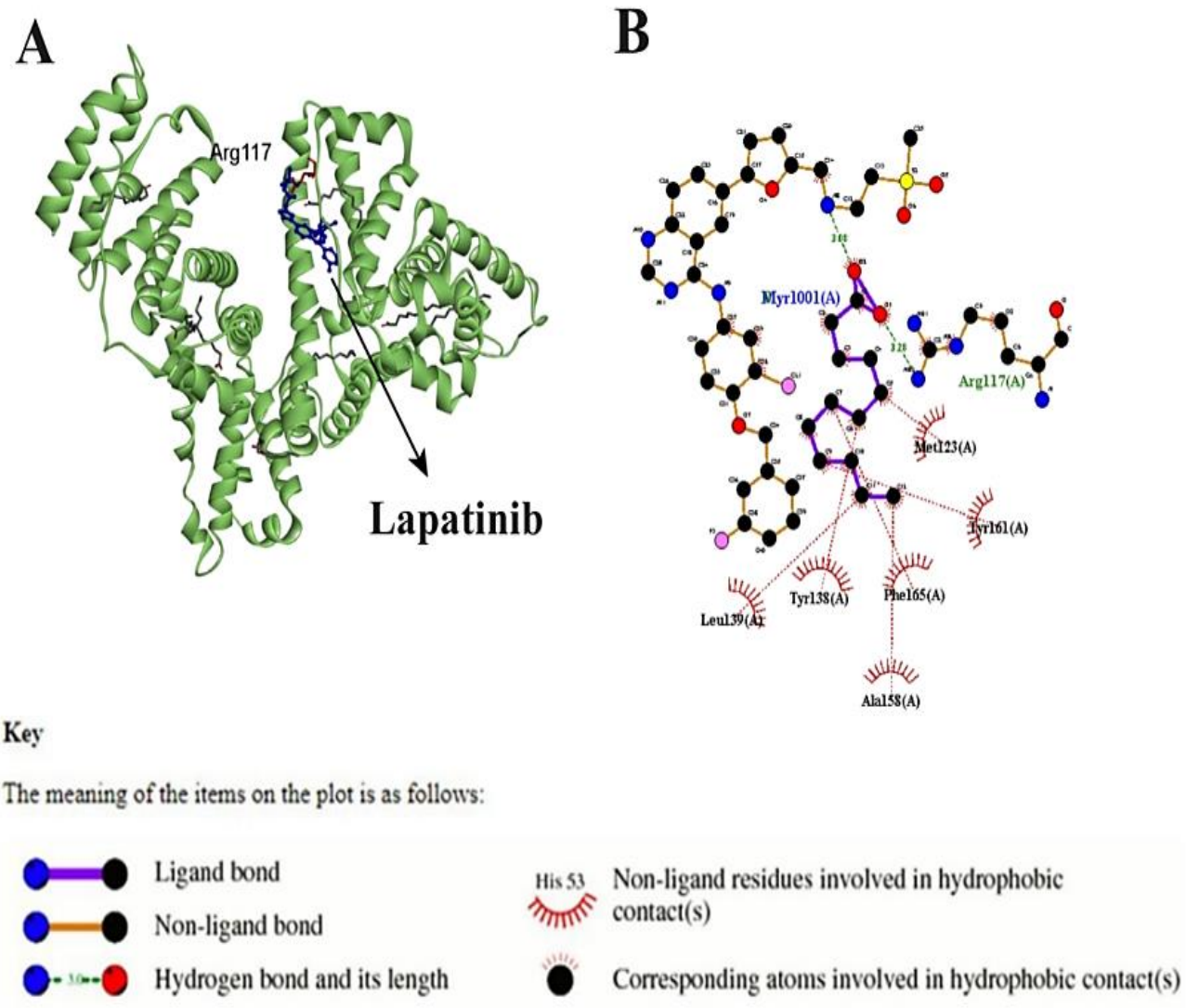


Figure 1. Docking of Lapatinib to HSA. Three-dimensional (left) and two-dimensional (right) representations show Lapatinib binding within the fatty acid pocket of HSA domain IB. Hydrogen bonds (Arg117) and hydrophobic contacts (Met123, Tyr161, Tyr138, Phe165, Ala158, Leu139) are highlighted.

[Downloaded from ijmcmed.org on 2026-11-07]

[DOI: 10.22088/IJMCM.BUMS.14.4.1031]

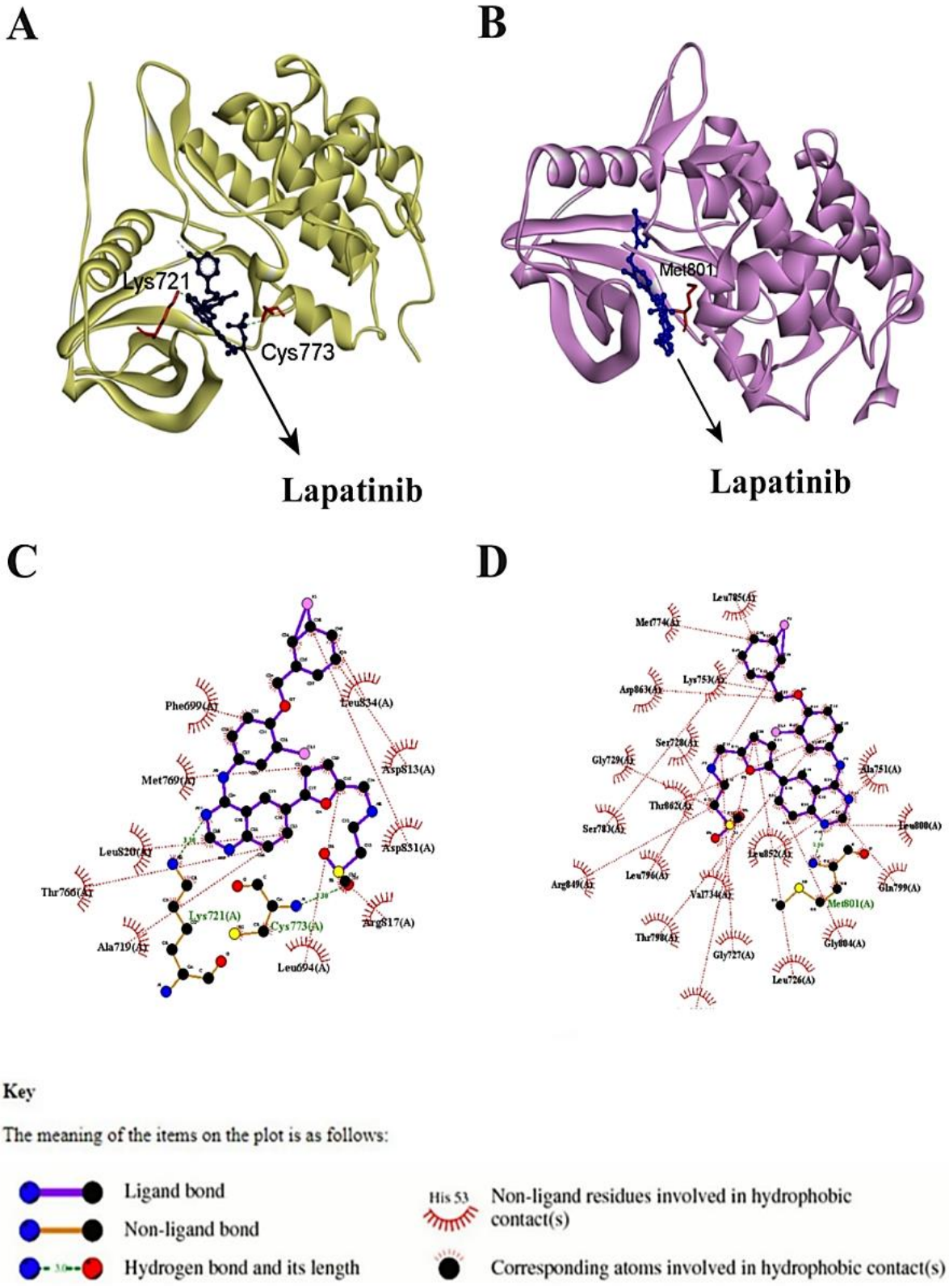


Figure 2. Three-Dimensional and Two-Dimensional Representations of Lapatinib Interactions with HER1 and HER2 Receptors. (A) and (C): Three-dimensional illustrations depict the interaction of Lapatinib with the active sites of the HER1 and HER2 receptors, respectively. (B) and (D): Two-dimensional diagrams, generated by Ligplot, show the hydrophobic and hydrogen bonding interactions between Lapatinib and the HER1 and HER2 receptors, respectively.

[Downloaded from ijmcmed.org on 2026-11-07]

[DOI: 10.22088/IJMCM.BUMS.14.4.1031]

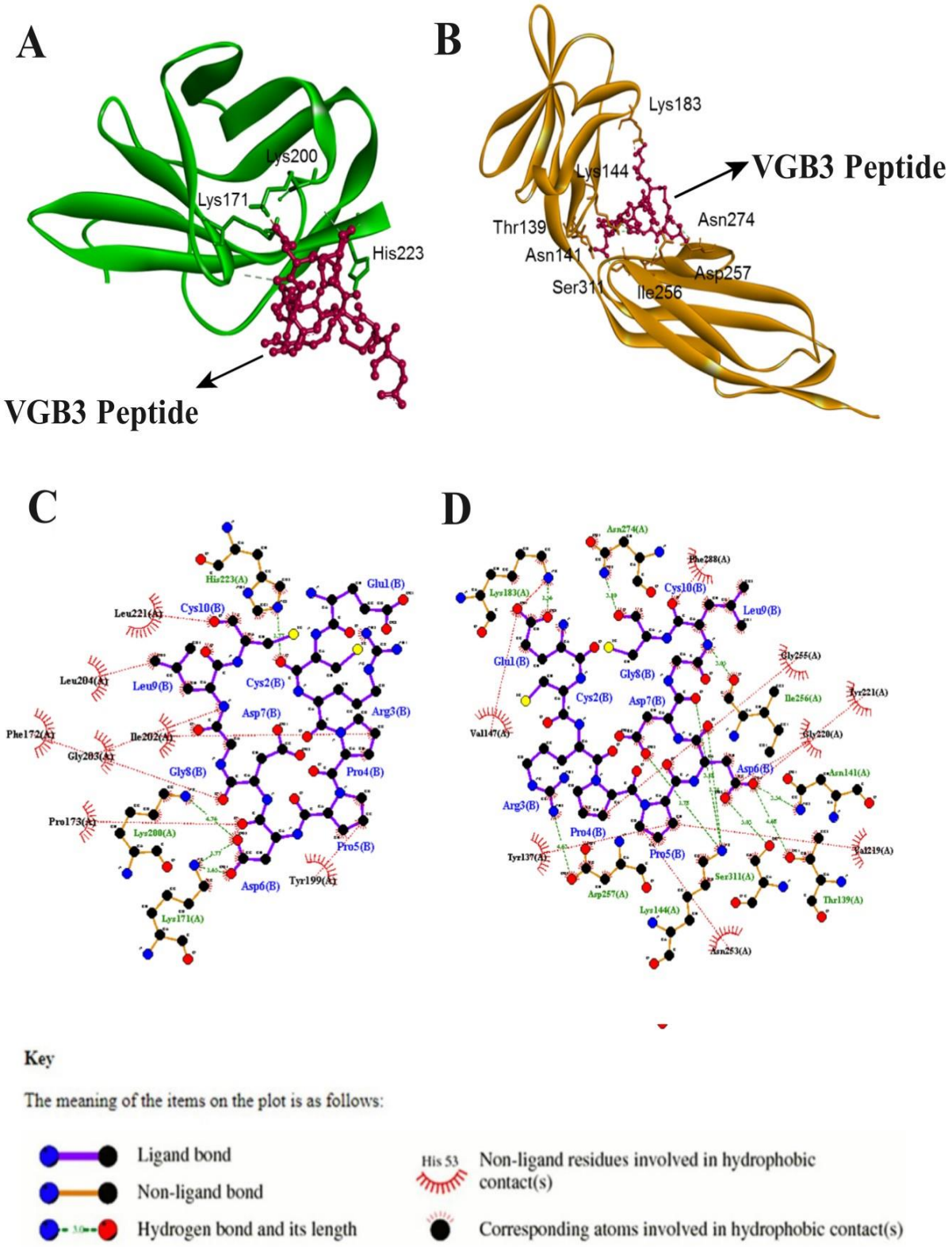


Figure 3. Three-dimensional and two-dimensional representations of the interaction between the VGB3 peptide and the VEGFR1 and VEGFR2 receptors. Panels A and C show the three-dimensional binding poses of the VGB3 peptide within the active sites of VEGFR1 and VEGFR2, respectively. Panels B and D present the two-dimensional interaction diagrams generated by LigPlot, illustrating the hydrophobic contacts and hydrogen bonds between the VGB3 peptide and VEGFR1 and VEGFR2, respectively.

[Downloaded from ijmcmed.org on 2026-11-07]

[DOI: 10.22088/IJMCM.BUMS.14.4.1031]

Table 1. UV-Vis Absorption Spectra of HSA-Lapatinib Complex before and After Dialysis for Determination of Lapatinib Concentration.

Sample	Absorbance at 368 nm
Lapatinib	1.1
HSA	0.0
HSA-Lapatinib Complex (before dialysis)	1.2
HSA-Lapatinib Complex (after dialysis)	0.8

The UV-Vis absorption spectra of the HSA-Lapatinib (HSA-LAP) complex were recorded before and after dialysis to assess the concentration of Lapatinib. After dialysis, only the HSA-LAP complex remained, and the concentration of Lapatinib was determined using a standard calibration curve at 368 nm.

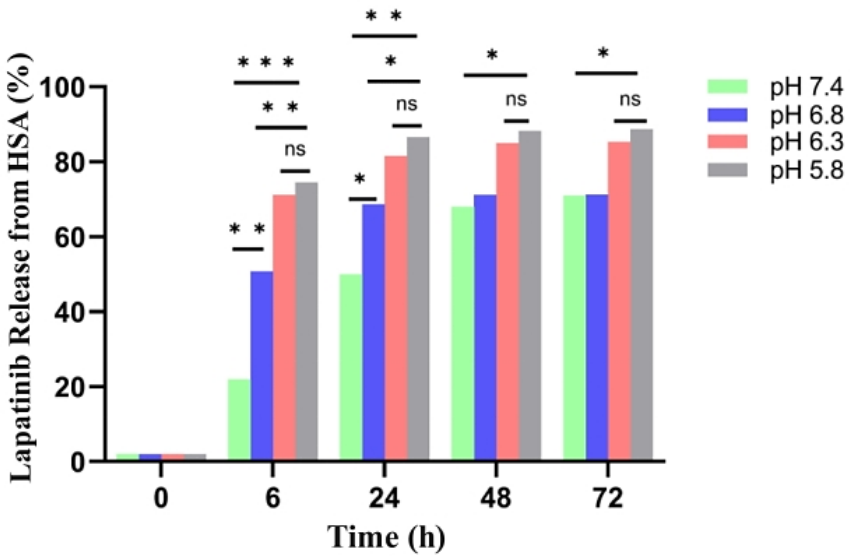


Figure 4. PH-dependent release of Lapatinib from HSA. Fluorescence emission at 428 nm was measured over 72 h at pH 5.8, 6.3, 6.8, and 7.4. Acidic conditions promote accelerated release. Data are mean ± SD (n = 3); one-way ANOVA with Tukey's post-hoc: *P < 0.05, **P < 0.01, ***P < 0.001, ***P < 0.0001; ns, not significant.

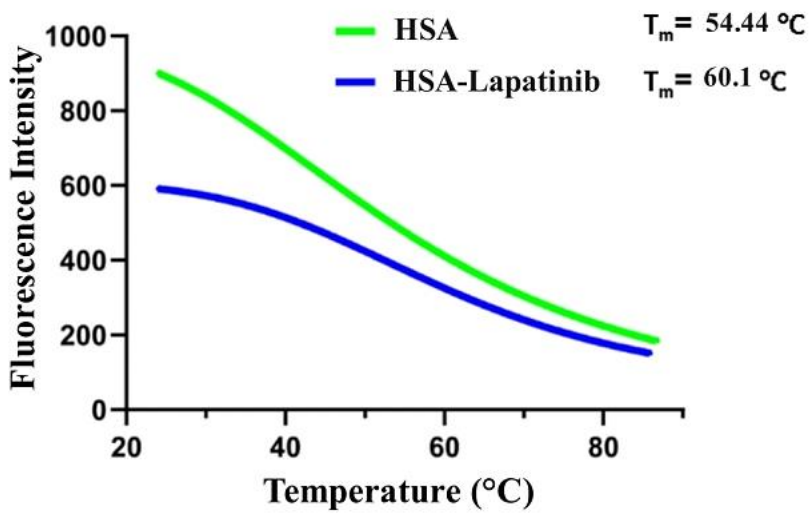


Figure 5. Thermal denaturation of HSA with and without Lapatinib. Lapatinib binding increases HSA's melting temperature by 5.5°C, indicating enhanced structural stability and conformational changes.

[Downloaded from ijmcmed.org on 2026-11-07]

[DOI: 10.22088/IJMCM.BUMS.14.4.1031]

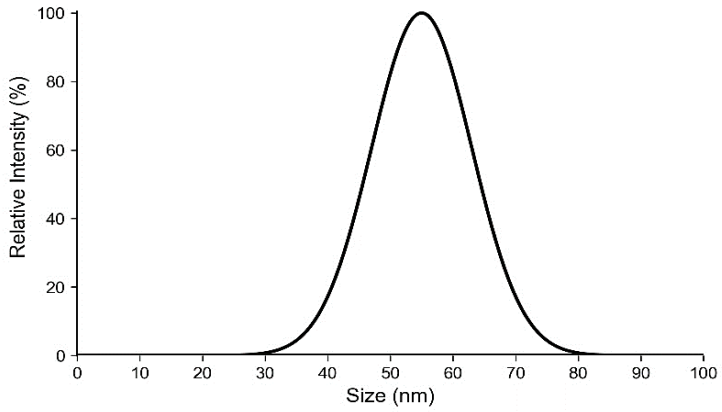


Figure 6. Mean hydrodynamic diameter of HSA–Lapatinib measured by DLS (~57 nm).

Cytotoxicity Assessment. **Cytotoxicity Assessment**

The comparative effects of Lapatinib and HSA–Lapatinib complexes on the viability of MDA-MB-231 breast cancer cells were systematically evaluated. HSA alone showed no cytotoxicity. MTT assay results indicated that Lapatinib exhibited IC_{50} values of 43.76 µM for free Lapatinib and 19.52 µM for the HSA–Lapatinib complex. The VGB3 peptide modestly reduced cell viability, showing approximately 80% with an IC_{50} value of 32 µM. Combination treatment with HSA–Lapatinib (17 µM) and VGB3 (0.18 µM) further reduced cell viability to 25% (Figure 7).

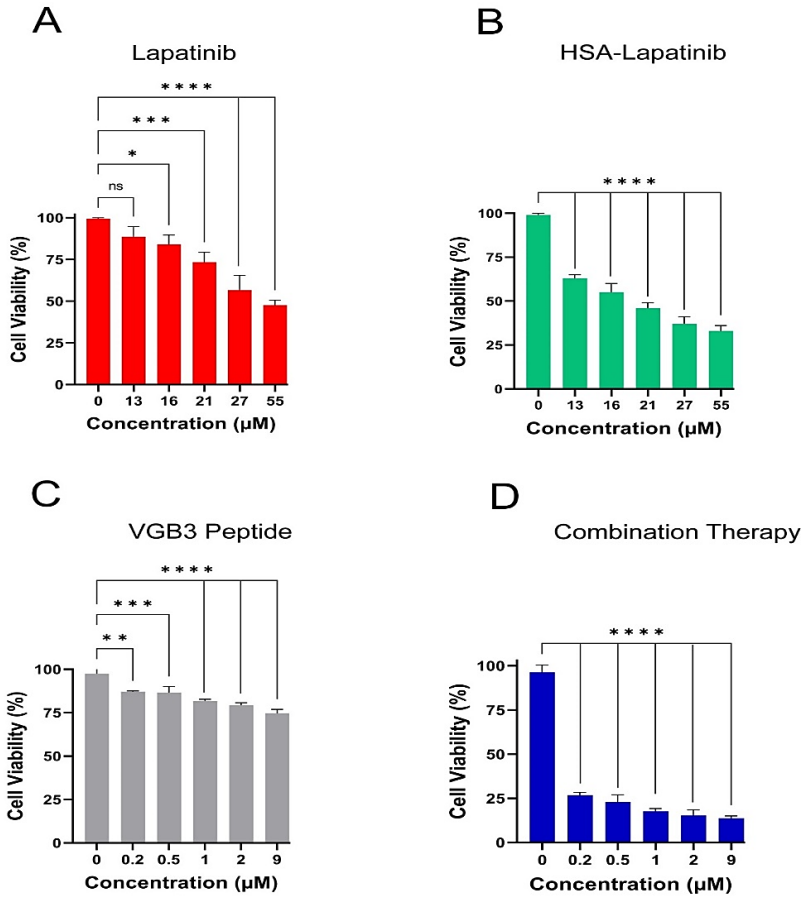


Figure 7. Cytotoxicity of HSA-Lapatinib and VGB3 peptide in MDA-MB-231 cells. Cell viability after 48 h treatment with Lapatinib, HSA-Lapatinib, VGB3 peptide, or combination therapy. The combination markedly reduced viability compared with either treatment alone. Data are mean ± SD (n = 3); ANOVA with Tukey post-hoc test.

[Downloaded from ijmcmed.org on 2026-11-07]

[DOI: 10.22088/IJMCM.BUMS.14.4.1031]

Synergistic Cytotoxicity of HSA–Lapatinib and VGB3 Combination

Treatment of MDA-MB-231 breast cancer cells with free Lapatinib and its HSA–Lapatinib complex demonstrated a dose-dependent reduction in cell viability, with IC_{50} values of 43.76 µM and 19.52 µM, respectively, confirming that albumin conjugation enhanced cytotoxic potency. The VGB3 peptide alone was relatively weak, producing about 80 % cell viability with an IC_{50} of 32 µM. Notably, the combination of HSA–Lapatinib (17 µM, below its IC_{50}) with VGB3 (0.18 µM, far below its active range) reduced viability to 25 %, equivalent to 75 % growth inhibition. Quantitative synergy assessment using the Chou–Talalay method yielded a Combination Index (CI) of 0.29 (< 1), establishing a true synergistic interaction between the two agents.

This synergy indicates that coupling Lapatinib to HSA improves intracellular availability, while VGB3 enhances receptor-mediated uptake, resulting in markedly greater anticancer efficacy at substantially lower doses than either agent alone.

Apoptosis Analysis

Annexin V/PI flow cytometry showed apoptosis in 40.8% of cells treated with HSA-Lapatinib and 34.5% with VGB3 alone. Combination treatment increased apoptosis to 46.8% ($P < 0.0001$), confirming enhanced pro-apoptotic activity compared with either treatment alone (Figure 8) (9).

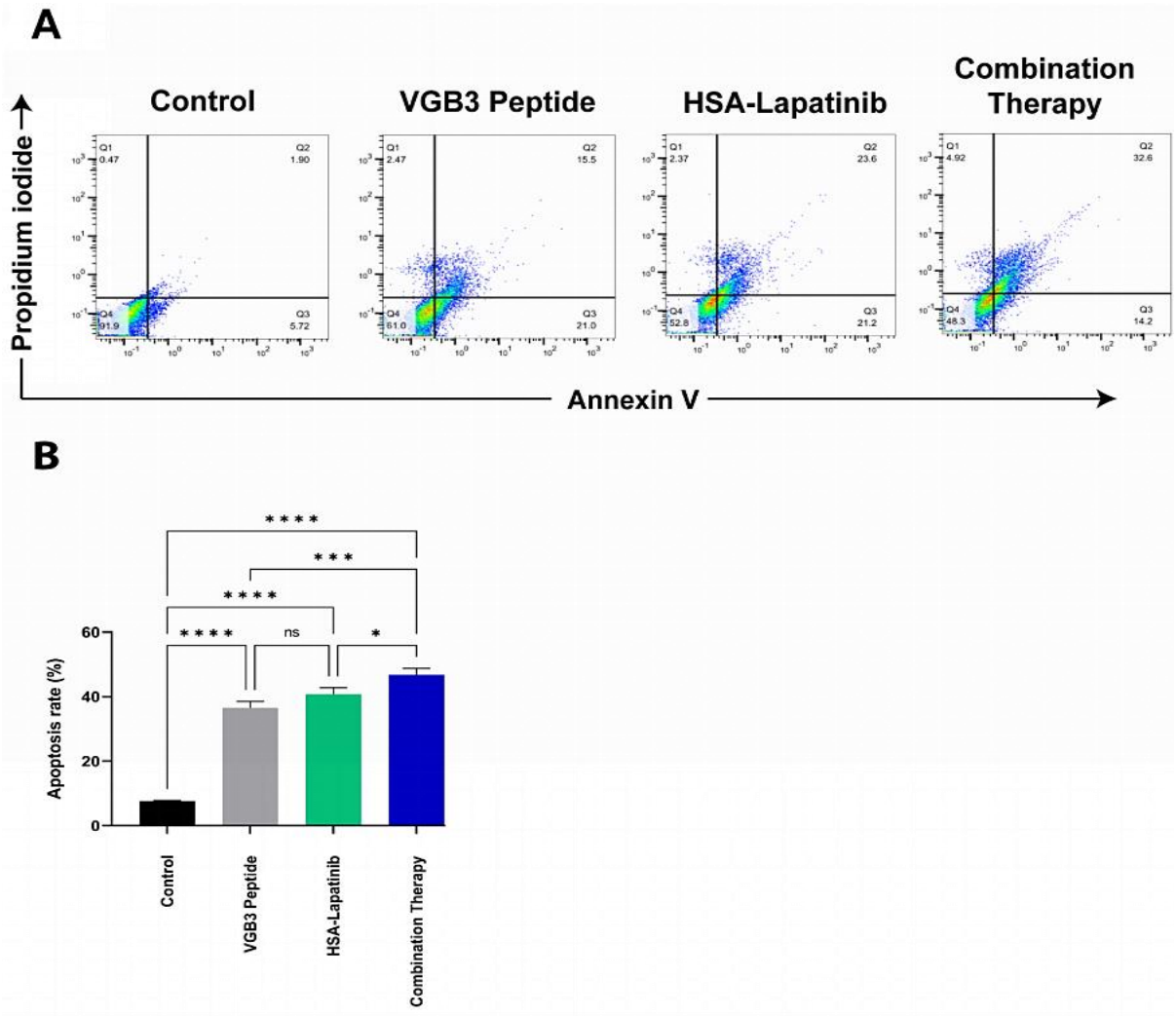


Figure 8. Apoptosis induction analysis. Apoptosis induction plots using Annexin V/PI staining in MDA-MB-231 cell line. A) and B) show treatments with VGB3 peptide, HSA-Lapatinib, and combination therapy (VGB3 peptide + HSA-Lapatinib). Statistical analysis was performed using one-way ANOVA, with significance levels denoted as *P < 0.05, **P < 0.01, ***P < 0.001, ****P < 0.0001, and ns indicating non-significance.

[Downloaded from ijmcmed.org on 2026-11-07]

[DOI: 10.22088/IJMCM.BUMS.14.4.1031]

Gene Expression Analysis

qPCR revealed that VGB3 peptide alone did not significantly alter VEGFR2 or VEGFA expression. In contrast, combination therapy increased VEGFR2 mRNA levels approximately fourfold compared to control ($P < 0.0001$) and modestly upregulated VEGFA ($P < 0.05$) (Figure 8). This pattern suggests that HSA-Lapatinib induces compensatory VEGFR2 upregulation, which is then targeted by VGB3, providing mechanistic support for the observed synergistic cytotoxicity (Figure 9).

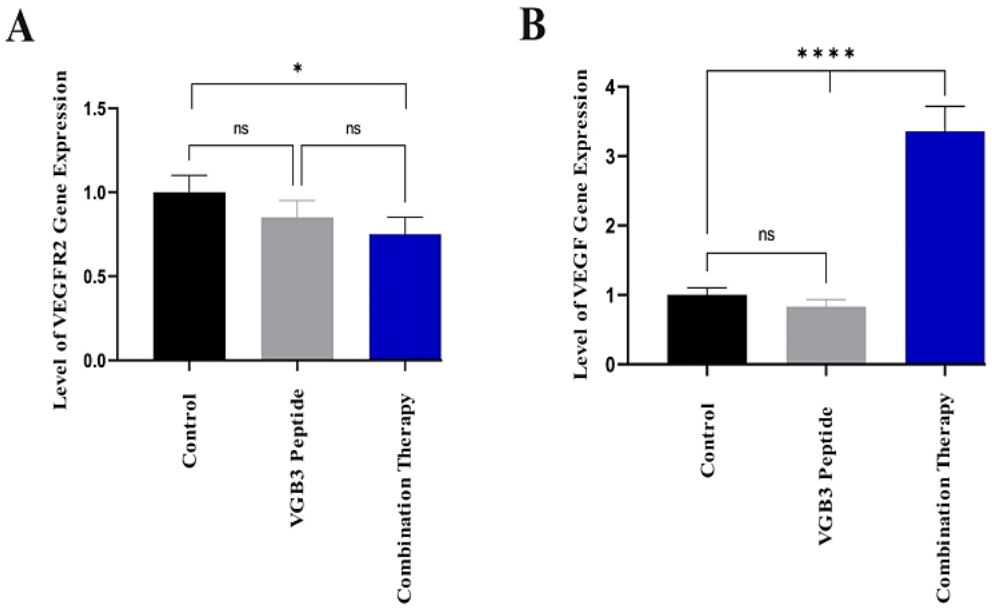


Figure 9. Expression of VEGF (A) and VEGFR2 (B) genes in MDA-MB-231 cell line treated with VGB3 peptide and combination therapy (VGB3 peptide and HSA-Lapatinib). Statistical analysis was performed using a one-way ANOVA test, and significance levels were set as P* < 0.05, P < 0.01, P*** < 0.001, P**** < 0.0001, and ns indicates non-significance.**

Discussion

This study suggests that loading Lapatinib onto HSA may provide a potentially effective therapeutic platform for TNBC, with indications of reduced toxicity. Lapatinib is a tyrosine kinase inhibitor with activity against TNBC and HER2-positive cancers, but its clinical utility is limited by poor aqueous solubility and off-target effects(32). Using HSA as a carrier enhances solubility, prolongs plasma half-life, and supports targeted accumulation in tumors via passive (EPR effect) and active pathways (SPARC/GP60) [8–10]. Our docking studies further confirmed strong interactions between Lapatinib and HSA, particularly in domain IB, supporting efficient drug loading.

Thermal stability data showed that Lapatinib binding increased the melting temperature (T_m) of HSA, indicating conformational stabilization of the protein–drug complex. Spectroscopic analyses confirmed both successful drug loading and pH-responsive release, with acidic conditions — mimicking tumor microenvironments — accelerating drug liberation. These findings align with earlier reports that nanoparticle-based systems can improve the delivery of hydrophobic agents in TNBC models. Notably, unlike many nanocarrier fabrication methods requiring toxic organic solvents, our approach avoids chloroform or dichloromethane, minimizing formulation-associated toxicity (33).

Comparative in vitro analyses revealed that the HSA–Lapatinib complex reduced cell viability more effectively than free Lapatinib, with a two-fold lower IC_{50}. The effect was further amplified when combined with VGB3 peptide, a selective VEGFR1/VEGFR2 inhibitor, producing statistically significant but modest decreases in viability and increases in apoptosis under in-vitro conditions.

This combination appears to extend previous observations, potentially through complementary VEGFR blockade that may target resistance pathways (34). Our work extends these findings by integrating VEGFR blockade to target resistance pathways.

[Downloaded from ijmcmed.org on 2026-11-07]

[DOI: 10.22088/IJMCM.BUMS.14.4.1031]

Gene expression results provide mechanistic insight: HSA–Lapatinib treatment triggered a compensatory four-fold increase in VEGFR2 expression — a potential survival mechanism for TNBC cells. VGB3 effectively neutralized this escape pathway, likely preventing VEGF-VEGFR2 signaling from sustaining angiogenesis despite HER pathway inhibition. This aligns with previous evidence that VEGF induction can upregulate VEGFR, making tumors more susceptible to VEGFR-targeting strategies (25, 27, 28). Our combination also modestly altered VEGFA expression, which may contribute to reduced angiogenic drive.

Overall, the data support a dual-targeting model in which HSA facilitates Lapatinib delivery and suppresses EGFR signaling, while VGB3 peptide mitigates the VEGFR2-dependent resistance loop.

The observed enhancements in tumor-targeting and cytotoxicity are consistent with our previously demonstrated in-vivo efficacy (9), reinforcing the translational relevance of this approach. Ongoing studies focus on comprehensive pharmacokinetic and mechanistic evaluations to further characterize synergy and safety profiles in complex biological models.

The present study highlights human serum albumin as an effective, biocompatible carrier for Lapatinib, offering enhanced solubility, prolonged stability, and pH-responsive release that favors tumor-specific drug delivery. Encapsulation in HSA not only reduced the IC_{50} compared with free Lapatinib, but also improved the therapeutic window by minimizing formulation-related toxicity.

Importantly, combining HSA-Lapatinib with the VEGFR1/VEGFR2-targeting peptide VGB3 produced potent synergistic activity against TNBC cells, driven by dual pathway inhibition. Mechanistically, HSA-Lapatinib induced a compensatory upregulation of VEGFR2, a resistance-linked escape mechanism that was effectively counteracted by VGB3, resulting in enhanced apoptosis and reduced cell viability. This dual-target approach represents a promising strategy for overcoming adaptive resistance in EGFR-driven, therapy-refractory cancers.

Future investigations should focus on in vivo validation, pharmacokinetic characterization, and broadening application to other solid tumors where parallel blockade of EGFR and VEGFR pathways may yield similar therapeutic benefit.

References

1. Lei S, Zheng R, Zhang S, et al. Global patterns of breast cancer incidence and mortality: A population- based cancer registry data analysis from 2000 to 2020. Cancer Commun. 2021;41(11):1183-94.
2. Haki M, Bayat R. Innovative Approaches for Molecular Targeted Therapy of Breast Cancer: Interfering with Various Pathway Signaling. Int J Mol Cell Med. 2025;14(1):533.
3. Li Y, Wang M, Zhi P, et al. Metformin synergistically suppress tumor growth with doxorubicin and reverse drug resistance by inhibiting the expression and function of P-glycoprotein in MCF7/ADR cells and xenograft models. Oncotarget. 2017;9(2):2158.
4. Raja Sharin RNFS, Khan J, Ibahim MJ, et al. Role of ErbB1 in the Underlying Mechanism of Lapatinib- Induced Diarrhoea: A Review. BioMed Res. Int. 2022;2022(1):4165808.
5. Wan X, Zheng X, Pang X, et al. Lapatinib-loaded human serum albumin nanoparticles for the prevention and treatment of triple-negative breast cancer metastasis to the brain. Oncotarget. 2016;7(23):34038.
6. Yuan H, Guo H, Luan X, et al. Albumin nanoparticle of paclitaxel (Abraxane) decreases while taxol increases breast cancer stem cells in treatment of triple negative breast cancer. Mol. Pharm. 2020;17(7):2275-86.
7. Wan X, Zheng X, Pang X, et al. Incorporation of lapatinib into human serum albumin nanoparticles with enhanced anti-tumor effects in HER2-positive breast cancer. Colloids Surf. B Biointerfaces. 2015;136:817-27.
8. Saremi Poor A, Davaeil B, Ramezanpour M, et al. Nanoparticle Albumin-Bound Bortezomib: Enhanced Antitumor Efficacy and Tumor Accumulation in Breast Cancer Therapy. Mol. Pharm. 2025;22(5):2482-93.
9. Rostaminasab S, Esmaeili A, Moosavi-Movahedi F, et al. Enhanced antitumor activity of lapatinib against triple-negative breast cancer via loading in human serum albumin. Int J Biol Macromol. 2024;282:136760.
10. Dömötör O, Pelivan K, Borics A, et al. Comparative studies on the human serum albumin binding of the clinically approved EGFR inhibitors

[Downloaded from ijmcmed.org on 2026-11-07]

[DOI: 10.22088/IJMCM.BUMS.14.4.1031]

gefitinib, erlotinib, afatinib, osimertinib and the investigational inhibitor KP2187. J. Pharm. Biomed. Anal. 2018;154:321-31.
11. Ji Q, Zhu H, Qin Y, et al. GP60 and SPARC as albumin receptors: key targeted sites for the delivery of antitumor drugs. Front. Pharmacol. 2024;15:1329636.
12. Schnitzer J, Oh P. Antibodies to SPARC inhibit albumin binding to SPARC, gp60, and microvascular endothelium. Am. J. Physiol. Heart Circ. Physiol. 1992;263(6):H1872-H9.
13. Cho H, Jeon SI, Ahn C-H, et al. Emerging albumin-binding anticancer drugs for tumor-targeted drug delivery: current understandings and clinical translation. Pharmaceutics. 2022;14(4):728.
14. Ansari MJ, Bokov D, Markov A, et al. Cancer combination therapies by angiogenesis inhibitors; a comprehensive review. Cell Commun. Signal. 2022;20(1):49.
15. Rahdari T, Mahdavimehr M, Ghafouri H, et al. Advancing triple-negative breast cancer treatment through peptide decorated solid lipid nanoparticles for paclitaxel delivery. Sci. Rep. 2025;15(1):6043.
16. Rahdari T, Ghafouri H, Ramezanpour S, et al. Design and Characterization of Peptide-Conjugated Solid Lipid Nanoparticles for Targeted MRI and SPECT Imaging of Breast Tumors. ACS Omega. 2025.
17. Chamani R, Asghari SM, Alizadeh AM, et al. Engineering of a disulfide loop instead of a Zn binding loop restores the anti-proliferative, anti-angiogenic and anti-tumor activities of the N-terminal fragment of endostatin: Mechanistic and therapeutic insights. Vasc. Pharmacol. 2015;72:73-82.
18. Chamani R, Asghari SM, Alizadeh AM, et al. The antiangiogenic and antitumor activities of the N-terminal fragment of endostatin augmented by Ile/Arg substitution: the overall structure implicated the biological activity. Biochim. Biophys. Acta, Proteins Proteomics. 2016;1864(12):1765-74.
19. Mahdavimehr M, Rahdari T, Nikfarjam N, et al. Development and application of dual-modality tumor-targeting SPIONs for precision breast cancer imaging. Biomaterials Adv. 2025;172:214236.
20. Xun X, Ai J, Feng F, et al. Adverse events of bevacizumab for triple negative breast cancer and HER-2 negative metastatic breast cancer: A meta-analysis. Front. Pharmacol. 2023;14:1108772.
21. Zafrakas M, Papasozomenou P, Emmanouilides C. Sorafenib in breast cancer treatment: A systematic review and overview of clinical trials. World J Clin Oncol. 2016;7(4):331.
22. V Rosca E, E Koskimaki J, G Rivera C, et al. Anti-angiogenic peptides for cancer therapeutics. Curr. Pharm. Biotechnol. 2011;12(8):1101-16.
23. Shoari A, Khodabakhsh F, Cohan RA, et al. Anti-angiogenic peptides application in cancer therapy; a review. Res. Pharm. Sci. 2021;16(6):559-74.
24. Sadremomtaz A, Kobarfard F, Mansouri K, et al. Suppression of migratory and metastatic pathways via blocking VEGFR1 and VEGFR2. J. Recept. Signal Transduct. 2018;38(5-6):432-41.
25. Namjoo M, Ghafouri H, Assareh E, et al. A VEGFB-based peptidomimetic inhibits VEGFR2-mediated PI3K/Akt/mTOR and PLCγ/ERK signaling and elicits apoptotic, antiangiogenic, and antitumor activities. Pharmaceuticals. 2023;16(6):906.
26. Sadremomtaz A, Mansouri K, Alemzadeh G, et al. Dual blockade of VEGFR1 and VEGFR2 by a novel peptide abrogates VEGF-driven angiogenesis, tumor growth, and metastasis through PI3K/AKT and MAPK/ERK1/2 pathway. BBA Gen. Subj. 2018;1862(12):2688-700.
27. Sadremomtaz A, Ali AM, Jouyandeh F, et al. Molecular docking, synthesis and biological evaluation of Vascular Endothelial Growth Factor (VEGF) B based peptide as antiangiogenic agent targeting the second domain of the Vascular Endothelial Growth Factor Receptor 1 (VEGFR1D2) for anticancer application. Signal Transduct. Targeted Ther. 2020;5(1):76.
28. Zanjanchi P, Asghari SM, Mohabatkar H, et al. Conjugation of VEGFR1/R2-targeting peptide with gold nanoparticles to enhance antiangiogenic and antitumoral activity. J. Nanobiotechnol. 2022;20(1):7.
29. Bejari M, Sasani ST, Asghari SM, et al. Vascular endothelial growth factor antagonist peptides inhibit tumor growth and metastasis in breast cancer through repression of c-src and STAT3 genes. Mol. Biol. Rep. 2023;50(11):9213-9.
30. Sudlow G, Birkett D, Wade D. The characterization of two specific drug binding sites

[Downloaded from ijmcmed.org on 2026-11-07]

[DOI: 10.22088/IJMCM.BUMS.14.4.1031]

on human serum albumin. Mol. Pharmacol. 1975;11(6):824-32.
31. Kabir MZ, Mukarram AK, Mohamad SB, et al. Characterization of the binding of an anticancer drug, lapatinib to human serum albumin. J. Photochem. Photobiol. B Biol. 2016;160:229-39.
32. Movagharnejad K, Sharbatdaran M, Sheffaee S, et al. HER-2/neu marker examination using immunohistochemical method in patients suffering from gastric adenocarcinoma. Int J Mol Cell Med. 2013;2(4):199.
33. Wan X, Zheng X, Pang X, et al. The potential use of lapatinib-loaded human serum albumin nanoparticles in the treatment of triple-negative breast cancer. Int J Pharm. 2015;484(1-2):16-28.
34. Zhang Z, Zhang J, Jiang M, et al. Human serum albumin-based dual-agent delivery systems for combination therapy: acting against cancer cells and inhibiting neovascularization in the tumor microenvironment. Mol. Pharm. 2020;17(4):1405-14.

[Downloaded from ijmcmed.org on 2026-11-07]

[DOI: 10.22088/IJMCM.BUMS.14.4.1031]